Wear 266 (2009) 621–626

Contents lists available at ScienceDirect

Wear

journal homepage: www.elsevier.com/locate/wear

On the behaviour of obsidian under scratch test

H. Ben Abdelounis [a], K. Elleuch [b,*], R. Vargiolu [a], H. Zahouani [a], A. Le Bot [a]

[a] Laboratoire de Tribologie et Dynamique des Systèmes, Ecole Centrale de Lyon, France
[b] Laboratoire des Systèmes Electro-Mécaniques, Ecole Nationale d'Ingénieurs de Sfax, Tunisia

ARTICLE INFO

Article history:
Received 2 January 2008
Received in revised form 11 June 2008
Accepted 9 July 2008
Available online 5 September 2008

Keywords:
Scratch
Obsidian
Crack
Toughness

ABSTRACT

This study deals with the mechanical characterization of three types of obsidian with scratch tests. These obsidians have been selected for their archeological interest and, in particular, they have been taken in three different sites in Turkey: Bingöl, Nenezi Dag and Kayirli.

Known as being brittle, the mechanical analysis of such material requires a special attention. The porosity is measured by optical method. The incremental scratch test is used to determine the critical normal load and the constant scratch test is used to determine the toughness. Two types of indenters, conical and spherical, have been used.

Three regimes of damage have been observed, the micro-ductile, the micro-cracking and the micro-abrasive regimes. It has been found that the obsidian from Nenezi Dag is more tough than the two others and, in the same time, that it has a lower porosity than the others.

1. Introduction

In archeology, use-wear analysis is today a well-accepted method intended to the identification of the usage of prehistoric tools, especially those made of stone. Astruc et al. [1] give several examples of the application of use-wear analysis on vessels, figurines or pendants which have led to a better understanding of the social organization of a neolithic population during the VII millennium B.C., in Cyprus.

The interest of ancient populations in brittle materials is well known. It is justified by their usefulness in several human activities, fishing, hunting, farming, cooking and many others. The need to cut, to pierce, to mince, to crush and so on, requires the control of brittle materials. These materials were certainly selected for their mechanical properties. Therefore, the mechanical characterization of these materials is an essential step to understand the choice of these materials. Forming part of natural glass families, the obsidians were exploited and adapted by prehistoric man to manufacture various tools.

The aim of this study is to propose a tribological characterization of prehistoric obsidian.

Scratch test is a technique which provides much information on wear mechanisms. The fundamental phenomena of sliding wear such as cracking, and chipping are reproduced in the scratch test. Since the 1980s, it is known that the study of scratching of brittle materials give the same information than an indentation test [2–4] concerning the cracking phenomenon. In particular, Swain [5] found that the occurrence of microfracturing during the scratching of brittle materials is very similar to the one that happens under quasi-static indentation excepted that in scratch test a tangential load is applied in addition to the normal load. Swain defines three regions for damage in glasses depending on the applied normal load: between 0 and 0.1 N the scratching is fully plastic, between 0.1 and 5 N, median and lateral cracks occur, and for higher loads median cracks and poorly developed lateral cracks are observed combined with a crushing track.

A commonly used sectioning technique to detect the subsurface damage is the bonded interface technique, where sections cut perpendicular to the scratch direction previously bonded by adhesive are viewed by scanning electron microscope (SEM) [6]. However, this technique does not lend itself to visualization of shallow subsurface damage occurring under low normal loads or brittle materials.

In this study, results of scratch tests on three types of obsidian selected for their archeological interest are presented. The cracking critical normal load, the toughness and the cracking modes are determined for two types of indenters.

* Corresponding author at: Laboratoire des Systèmes Electro-Mécaniques, Ecole Nationale d'Ingénieurs de Sfax, BP. W. 3038 Sfax, Tunisia. Tel.: +216 74 274 088; fax: +216 74 275 595.
E-mail address: khaled.elleuch@enis.rnu.tn (K. Elleuch).

0043-1648/$ – see front matter © 2008 Elsevier B.V. All rights reserved.
doi:10.1016/j.wear.2008.07.007

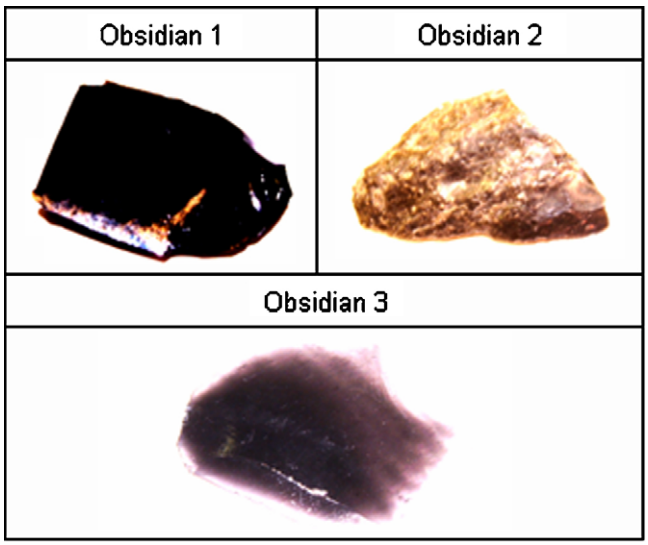

Fig. 1. Optical photo of the three obsidians: obsidian 1 from Bingöl, obsidian 2 from Nenezi and obsidian 3 from Kayirli.

Table 1
Measurement of the surface porosity

Material	Porosity (%)
Obsidian 1	18
Obsidian 2	10
Obsidian 3	13

2. Experimental

2.1. Materials

Obsidian has a volcanic origin. This is an amorphous material which consists of approximately an equal proportion of quartz (SiO_2), orthose (Si_3AlO_8K) and albite (Si_3AlO_8Na).

Three obsidians are tested. They have different colours (Fig. 1) since they have different geographical origins. Obsidian 1 comes from Bingöl which is located in Eastern Anatolia (actual Turkey). Obsidian 2 comes from Nenezi Dag area located in Central Anatolia. Finally, obsidian 3 comes from Kayirli (near Göllü Dag volcano also in Central Anatolia).

The porosity was measured by an optical profiler (Wyko NT109597). The vertical resolution is 2 nm and the horizontal resolution is less than 1 μm. Results are presented in Table 1. It is found that obsidian 1 (Ob1) has the biggest porosity value.

Samples used in scratch tests are enrobed and polished from P400 to P4000.

2.2. Scratch test

The scratch tester used in this study was developed in Ecole Centrale de Lyon in order to perform scratch experiments under various loads or penetration depth. All the characteristics of the scratch tester are presented in Ref. [7] and in Table 2. The normal load F_n, the penetration depth h and the tangential force F_t are continuously measured during the experiment.

Table 2
Sclerometer capacities

Range of normal force (F_n)	0–50 N
Range of tangential force F_t	0–20 N
Range of scratch length L	0.5–10 mm
Scratch speed	50–2500 μm/s

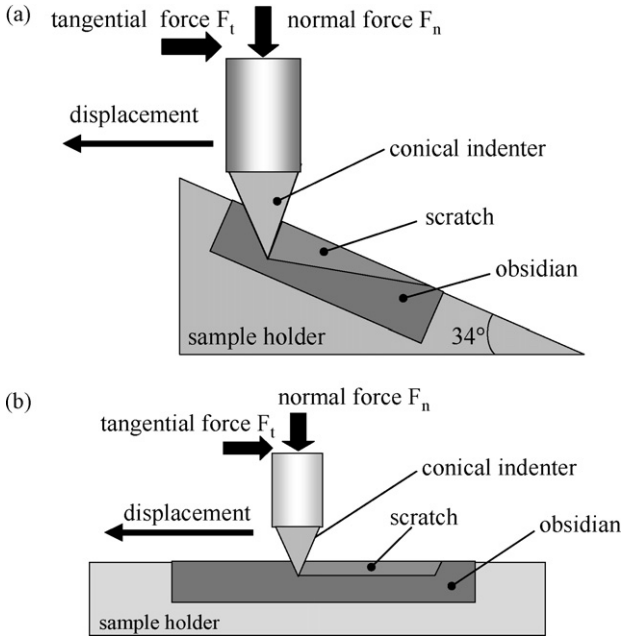

Fig. 2. Scratch test configurations: (a) incremental scratch and (b) constant scratch.

Two configurations of scratch test have been used: scratch test with increasing normal load and scratch test with constant normal load.

2.2.1. Scratch test with increasing normal load–incremental scratch

In this case, the sample is tilted with a predefined slope. Fig. 2(a) shows the principle of this test. After the indentation phase is done (imposing an initial normal load, F_{n0}), the sample is moved in the sliding direction and the normal load increases proportionally to the sliding distance. When the desired scratch length is reached, the indenter rises (in the vertical direction) and then the sample moves back without contact with the indenter. This is a single pass scratch test. If a multipass test is desired, the previous process is repeated as many times as required, so that a superimposed scratch scar is realized.

2.2.2. Scratch test with constant normal load–constant scratch

Fig. 2(b) shows the principle of this scratch test. It differs from the previous one by the fact that the sample is now positioned in such a way that its surface is parallel to the sliding direction of the indenter. In this configuration, the normal force is maintained constant during the test.

In all performed scratch tests, the sliding speed is 250 μm/s. For incremental scratch test, the sliding distance is 10 mm. But for constant scratch test, the sliding distance is only 2 mm in order to ensure a constant normal load.

Two indenters have been used: conical and spherical indenters. The spherical indenter has a radius of 2 mm and is made of steel 100Cr6 (1% of carbon and 1.5% of chrome). The conical indenter is made of diamond. The semi-angle is 120° and the radius of curvature of its vertex is 5 μm.

In all incremental scratch tests with conical indenter of this study, the angle of inclination between the obsidian surface and the sliding direction is 34° and the initial normal load is F_{n0} = 0.1 N. But with the spherical indenter, the angle of inclination is 68° and the initial normal load is F_{n0} = 20 N.

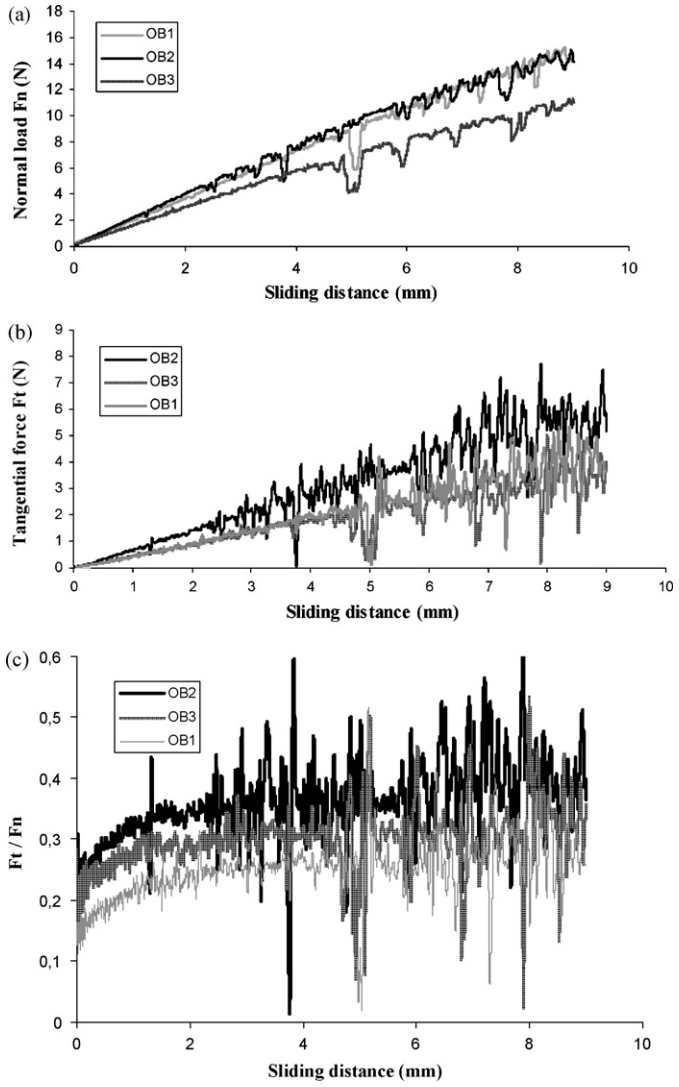

Fig. 3. Forces versus sliding distance in incremental scratch using conical indenter: (a) normal load F_n, (b) tangential force F_t and (c) ratio F_t/F_n.

3. Results and discussion

3.1. Incremental scratch with conical indenter

Fig. 3(a) shows the linear variation of normal force versus the sliding distance during the incremental scratch tests of the three obsidians, whereas Fig. 3(b) shows the tangential force versus the sliding distance.

Ob3 gives rise to a lower normal load than Ob1 and Ob2. However, Ob2 has the highest values of tangential force. This explains the higher ratio F_t/F_n of Ob2 shown in Fig. 3(c).

It can be noted that the evolution of forces is first regular for low loads and, above a certain sliding distance, i.e. a critical normal load, some fluctuations appear. Furthermore, these unstable variations are more and more important for high normal loads. This behaviour can be observed on both forces in Fig. 3(a) and (b) and is attributed to the apparition of chips and the presence of surface defaults (porosity, roughness, etc.).

The observation of the scratches illustrates three zones shown in Fig. 4(a):

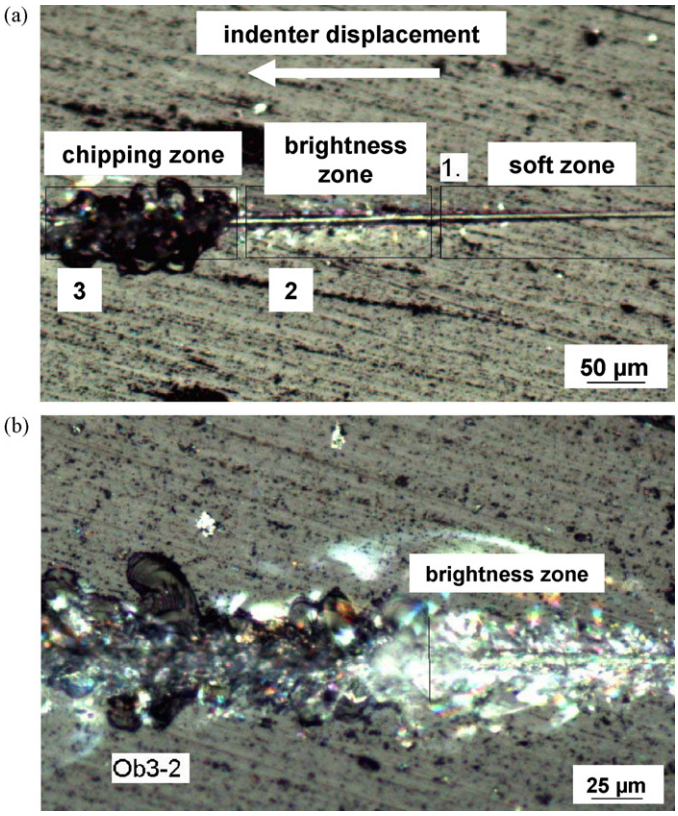

Fig. 4. Optical photo of the obsidian 3 under incremental scratch: (a) illustration of three zones and (b) detail of the brightness zone.

- The first zone is a "soft zone" where the aspect of the scratch has a regular morphology. It corresponds to low normal load values. This is the micro-ductile regime which consists on a permanent scratch track without damage on both sides and without visible debris.
- The second zone is a "brightness zone" where cracks appear without forming chips (Fig. 4(b)). This zone exhibits a brilliant aspect. The cracks start under the surface and sometimes, reach the surface. Two types of cracks are present, lateral cracks and radial cracks. This is the micro-cracking regime characterized by an important damage by micro-cracking.
- The third zone, the "chipping zone", corresponds to the formation of chips and many other debris. It appears for high normal load values. In this zone, there is a crack network, radial cracks and lateral cracks intersecting the surface. This zone is the most damaged part and leads to an irregular morphology of the edge of the scratch scar. This is the micro-abrasive regime.

These observations well agree with those of Swain [5]. It is important to note that the apparition of fluctuations on F_n and F_t can be strongly correlated to the scratch facies. Thus, the critical threshold of normal load (F_{nc}) can be defined as the force separating the second zone and the third zone. For $F_n < F_{nc}$ the scratch maintains a quasi-regular shape which explains the regularity of force signals. But when the transition occurs for $F_n \geq F_{nc}$, the apparition of chipping phenomenon occurs and consequent fluctuations in F_n and F_t will appear.

In practice, the total length d of the second and the third zone is measured and is reported in the curve $F_n = f(d)$ to deduce F_{nc}. For each obsidian the incremental scratch test was repeated eight times to confirm the value of F_{nc}. Results are presented in Table 3.

Table 3
Critical loads

Samples	Ob1		Ob2		Ob3	
	Critical, F_n (N)	Corresponding, F_t (N)	Critical, F_n (N)	Corresponding, F_t (N)	Critical, F_n (N)	Corresponding, F_t (N)
1	1.1	0.3	1.1	0.28	0.9	0.22
2	1.3	0.38	0.9	0.24	0.9	0.2
3	1.2	0.33	0.7	0.18	0.8	0.18
4	1.2	0.33	1	0.25	0.8	0.21
5	1.2	0.22	0.9	0.24	0.8	0.21
6	1.1	0.22	0.9	0.27	0.5	0.1
7	1	0.18	0.7	0.22	1.0	0.26
8	0.9	0.2	0.8	0.26	0.8	0.2
Average	1.1 ± 0.2	0.27	0.9 ± 0.2	0.24	0.8 ± 0.2	0.20

It is found that obsidian 1 has the highest value of critical normal load, whereas the two others have similar values.

3.2. Constant scratch test with conical indenter

In Fig. 5(a) the typical scratch pattern obtained under the critical normal load in the incremental scratch test is shown. In spite of the cracking of the obsidian, the width of the scratch remains almost constant with a rather significant depth (40 μm). However, it presents random degradations shown in Fig. 5(b) that may be classified as follows.

The wear debris is a powder which particles are of order of few micrometers (Fig. 5(b)). Evans and Marshall [8] report that the lateral cracking dominates the material removal in brittle material and is then of major interest for the understanding of machining processes.

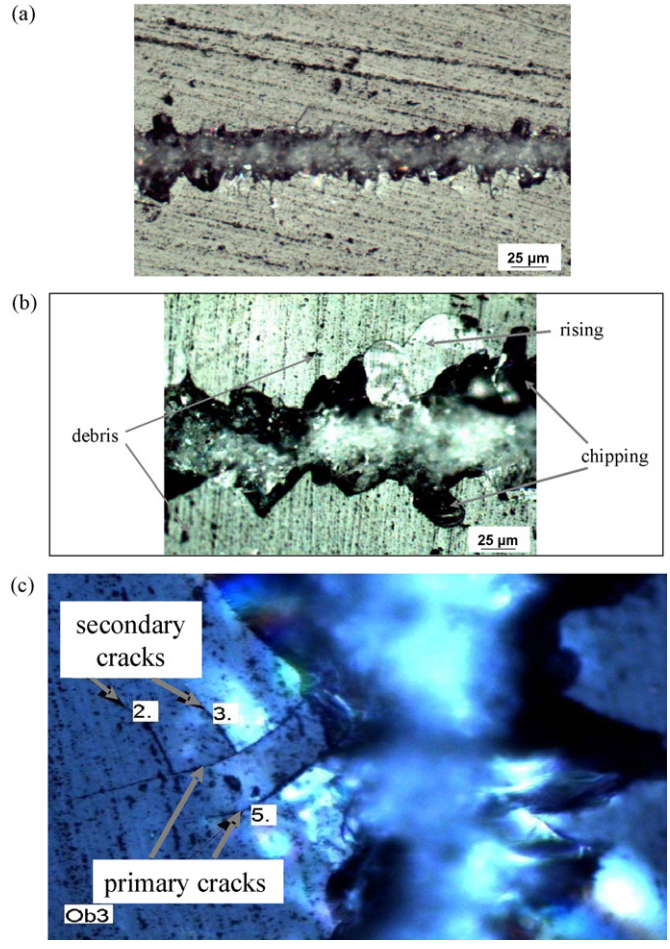

Fig. 5. (a) Scratch pattern in constant scratch (F_{nc}) of obsidian 3; (b) illustration of chipping, rising and debris formation; (c) primary and secondary cracks.

The matter rising is the mechanism that precedes chipping but without matter removal. Marshall et al. [9] point out a dynamical phenomenon during scratching reported in a section view along the scratch. It shows that the median crack does not propagate like one long and unique median crack but like successive median cracks that are created all along the scratch.

The chipping leads to the removal of large pieces of matter. Le Houérou et al. [10] explains that chipping occurs when the lateral cracks propagate from the indenter vertex towards the specimen surface and reach the surface.

The cracking may be of different types visible throughout the scratch. The primary cracks directly start from the scratch and secondary cracks start from primary cracks. It should be noted that these secondary cracks are short. The primary cracks propagate from the zone of the contact on the surface, in a vertical plane with the direction of the scratching, and emerge on the surface. Whereas the secondary cracks have an orthogonal direction with that of the primary cracks (Fig. 5(c)). In Table 4 the mean crack lengths obtained from a direct measurement through a microscope. We note that obsidian 1 has the biggest cracking average length, whereas the two others have a similar crack length (Table 4). It can be also noted that these averaged crack lengths observed on the samples well agree with the measurement of the porosity; the less porous being obsidian 2 (Nenezi) with small crack lengths, then obsidian 3 (Kayirli) and finally the most porous is obsidian 1 (Bingöl) with the largest cracks.

To compare the toughness of the three obsidians, the cracking frequency is considered. The cracking frequency is defined as the number of cracks per unit scratch length

$$f = \frac{N}{L} \quad (1)$$

where N is the total number of cracks and L is the scratch length. This cracking frequency can also be expressed in Hz by multiplying it by the sliding speed. Results are shown in Table 5. A high cracking frequency is related to a more fragile behaviour such as in the case of obsidian 1. Hence, obsidian 2 has the less fragile behaviour.

The calculation of toughness can be done as follows. Since the cone is moving and therefore is in contact only over its front face, the contact area is reduced to the surface of the front half-cone. The

Table 4
Average lengths of the cracks

	a_m (μm)
Ob1	40 ± 2
Ob2	28 ± 3
Ob3	30 ± 2

Table 5
Frequency of cracking

Material	N_m	$f(mm^{-1})$	$f(Hz)$
Ob1	210	21	5.25
Ob2	112	11	2.75
Ob3	143	14	3.5

Table 6
Critical normal stress and toughness

Material	F_{nc} (N)	D_m (μm)	σ_{nc} (MPa)	K_c (MPa $m^{1/2}$)
Ob1	1.1	41.5	1666	1.21
Ob2	0.9	29.5	2596	1.62
Ob3	0.8	32	2000	1.3

normal stress is equal to the normal force divided by the relevant surface that is the actual contact area of the half-cone projected on the surface plane. If the mean scratch width is noted D_m, the normal projected contact area is $\pi D_m^2/8$. The critical normal stress σ_{nc}, that is the stress which gives rise to cracks, is equal to the ratio of the critical normal load F_{nc} and the normal contact area $\pi D_m^2/8$:

$$\sigma_{nc} = \frac{8F_{nc}}{\pi D_m^2} \quad (2)$$

During the sliding, the stress σ is maximum at the back edge of the contact where the cracks start.

Following Griffith's theory of the cracking of brittle materials [11] in mode I under traction, the stress σ is related to the crack length a by

$$\sigma = \frac{K_c}{\sqrt{\pi a}} \quad (3)$$

where K_c is the toughness. But in scratch test, the cracks are initiated under compression instead of traction. The rupture under compression is not controlled by the propagation of a single crack, but by the propagation of many cracks in the crushing zone [12]. It is therefore more relevant to consider the average length a_m of the cracks [13] in Eq. (3). Furthermore, for brittle materials, the compressive strength is greater than the tensile strength. The factor 15 is usually admitted [14]. The modified Griffith's relationship is then

$$\sigma_{nc} = 15\frac{K_c}{\sqrt{\pi a_m}} \quad (4)$$

The toughness K_c can now be obtained from Eq. (4):

$$K_c = \frac{\sigma_{nc}}{15}\sqrt{\pi a_m} \quad (5)$$

where a_m is the average length of the cracks directly measured on the sample and summarized in Table 4. Table 6 shows that obsidian 2 is the toughest one, whereas the lowest toughness appears for obsidian 1. Such results confirm the previous ones based on the cracking frequency.

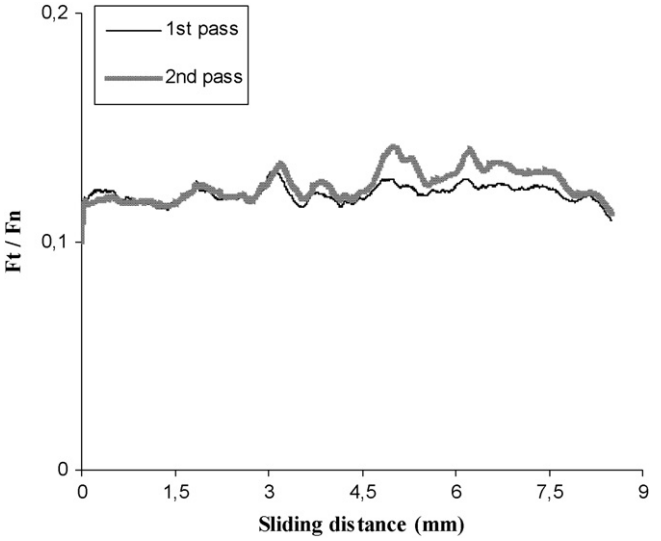

Fig. 6. Evolution of the ratio F_t/F_n versus sliding distance in incremental scratch of obsidian 2 using spherical indenter (F_{nc} = 20 N, 68°).

The measurement of the Vickers hardness show that obsidian 3 (Kayirli) is harder, 7.4 GPa, than the two others, 5.8 GPa for obsidian 1 (Bingöl) and 6.7 GPa for obsidian 2 (Nenezi). These results show that the brittleness (the opposite of toughness) does not follow the hardness. In this case, the less tough obsidian would be obsidian 3. The brittleness rather follows the porosity (the more porous being the less tough).

3.3. Incremental scratch tests with spherical indenter

In this section, the effect of the indenter geometry is investigated. A spherical indenter which radius is 2 mm has been used. But with the same conditions than the conical indenter, titled angle 34° and F_{n0} = 0.1 N, no damage is observed. Therefore, the tilted angle has been increased up to 68° and the initial normal force up to F_{n0} = 20 N.

Fig. 6 shows the evolution of F_t/F_n ratio of Ob2 (68° and F_{n0} = 20 N). No important fluctuations are noted and the ratio F_t/F_n tends to have a very low value (about 0.1). The first pass does not lead to any apparent damage on the surface neither under the surface. However, as remarked in Ref. [15], the maximal shear stress is localized under the surface and therefore, a residual stress is stored under the surface. The second pass gives rise to a magnification of the fluctuations of the force for obsidian 2 (Fig. 6). But this phenomenon is not sufficient to create incipient cracks on the surface.

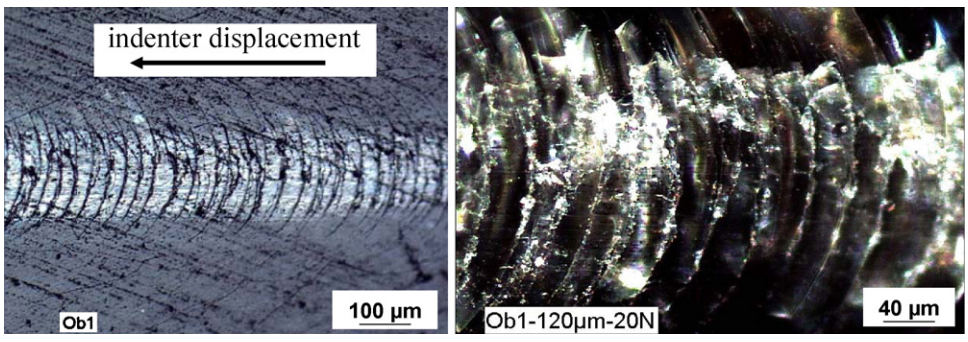

Fig. 7. Optical photo of Hertzian cracks of obsidian 1 for two incremental scratch passes (F_{nc} = 20 N, 68°).

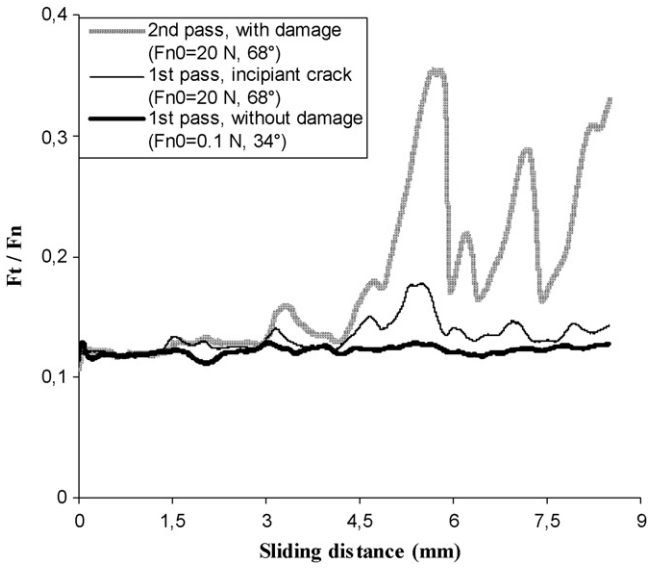

Fig. 8. Evolution of the ratio F_t/F_n versus sliding distance in incremental scratch of obsidian 1 using spherical indenter.

This result confirms the high toughness of obsidian 2. The critical normal load is certainly higher than the cell capacity (Table 2).

In contrast, when scratching Ob1 and Ob3 having lower toughness, a surface damage is found. Optical analyses highlight that Hertzian cracks (semi-circular cracks centered in the contact line and perpendicular to it) are created during the second incremented scratch pass (Fig. 7).

Fig. 8 shows that under a single pass (titled angle 34° and $F_{n0} = 0.1$ N) no damage is observed and the related friction coefficient is about 0.1. But, when the titled angle is 68° and $F_{n0} = 20$ N, subsurface cracks are generated under a single pass and the friction coefficient is first maintained to 0.1 and then slightly increased to 0.12 after a sliding distance of 4.5 mm when F_{nc} is reached ($F_{nc} = 35$ N for Ob1 and $F_{nc} = 30$ N for Ob3). Some fluctuations of F_n and F_t are then found. During the second pass (68° and $F_{n0} = 20$ N), these fluctuations become higher and simultaneously some cracks appear on the surface (Fig. 7). The related friction coefficient is located between 0.15 and 0.35.

Similar results were found by Ahn [16] and Bulsara [17,18] when considering monotonic loading/unloading cycles using a Vickers indenter. According to these authors three different regimes are typically observed: (i) the first one is associated with a permanent groove with eventually the formation of subsurface lateral cracks under the plastic track, and corresponds to a micro-ductile regime; (ii) the second one, so-called cracking regime, is characterized by an important damage by micro-cracking (lateral cracks intersecting the surface and radial cracks) and (iii) the third one is a micro-abrasive regime and gives birth to many debris, with sometimes small lateral cracks along the track.

4. Conclusion

The optical measurements and scratch tests on three types of obsidian, which all present a brittle behaviour, allow the following conclusions.

Three zones on the scratch scar have been identified depending on the values of F_n in the incremental scratch test:

- The micro-ductile zone in which there is no damage.
- The micro-cracking zone where subsurface cracks appear but without any chipping.
- The micro-abrasive zone with chipping and much debris in addition to emerging cracks.

It exists a critical normal load F_{nc} under which there is no chipping of the obsidian (separation of zones 2 and 3). The detection of F_{nc} (chipping apparition) has been made with the incremental scratch test by a direct observation of the apparition of chipping in the scratch scar and by substituting the sliding length in the $F_n - d$ diagram.

The toughness has been evaluated with the constant scratch test by considering the cracking frequency and its value K_c has been calculated by applying Griffith's theory. Obsidian from Nenezi Dag (Ob2) is the toughest one.

Using the spherical indenter, Hertzian cracks have been found. Furthermore, a second pass scratch shows that subsurface matter rises up to the surface even under low normal load. Without damage, the friction coefficient is maintained about 0.1 but it can reach 0.35 when chipping and cracking occur.

References

[1] L. Astruc, R. Vargiolu, H. Zahouani, Wear assessments of prehistoric instruments, Wear 255 (2003) 341–347.
[2] B.R. Lawn, A.G. Evans, D.B. Marshall, Elastic/plastic indentation damage in ceramics: the median/radial crack system, J. Am. Ceram. Soc. 63 (1980) 574–581.
[3] B.R. Lawn, M.V. Swain, Microfracture beneath point indentations in brittle solids, J. Mater. Sci. 10 (1975) 113–122.
[4] B.R. Lawn, E.R. Fuller, Equilibrium penny-like cracks in indentation fracture, J. Mater. Sci. 10 (1975) 2016–2024.
[5] M. Swain, Microfracture about scratches in brittle solids, Proc. R. Soc. Lond. A 366 (1979) 575–597.
[6] A.K. Mukhopadhyay, D. Chakraborty, M.V. Swain, Y.-W. Mai, Scratch deformation behaviour of alumina under a sharp indenter, J. Eur. Ceram. Soc. 17 (1997) 91–100.
[7] S. Ducret, C. Pailler-Mattéi, V. Jardret, R. Vargiolu, H. Zahouani, Friction characterisation of polymers abrasion (UHWMPE) during scratch tests: single and multi-asperity contact, Wear 255 (2003) 1093–1100.
[8] A.G. Evans, D.B. Marshall, Fundamentals of Friction and Wear materials, American Society of Metals, Metals Park, Ohio, USA, 1980, p. 439.
[9] D.B. Marshall, A.G. Evans, B.T. Khuri Yakub, J.W. Tien, G.S. Kino, The nature of machining damage in brittle materials, Proc. R. Soc. Lond. A 385 (1983) 461–475.
[10] V. Le Houérou, J.-C. Sangleboeuf, T. Rouxel, Scratch ability of soda–lime silica (SLS) glasses: dynamic fracture analysis, Key Eng. Mater. 290 (2005) 31–38.
[11] A.A. Griffith, The theory of rupture, in: Proceedings of the International Congress for Applied Mechanics, Delft, 1924.
[12] V. Jardet, H. Zahouani, J.L. Loubet, T.G. Mathia, Understanding and quantification of elastic and plastic deformation during a scratch test, Wear 218 (1998) 8–14.
[13] J.M. Georges, Frottement, usure et lubrification: La Tribologie ou science des surfaces, CNRS Editions, France, 2000.
[14] M.F. Ashby, D.R. Jones, Engineering Materials, Pergamon Press, Oxford, 1980.
[15] K.L. Johnson, Contact Mechanics, Cambridge University Press, 1985.
[16] Y. Ahn, Deformation about sliding indentation in ceramics and its application to lapping, Ph.D. thesis, Purdue University, USA, 1992.
[17] V.H. Bulsara, Scratch formation in brittle solids and its application to polishing, Ph.D. thesis, Purdue University, USA, 1997.
[18] V.H. Bulsara, Direct observation of contact damage around scratches in brittle solids, in: R.W. Tustison (Ed.), Proceedings of SPIE, Window and Dome Technologies and Materials V, vol. 3060, 1997, pp. 76–88.